NJC

# Green synthesis of gold, silver, platinum, and palladium nanoparticles reduced and stabilized by sodium rhodizonate and their catalytic reduction of 4-nitrophenol and methyl orange


| | |
|---|---|
| Journal: | *New Journal of Chemistry* |
| Manuscript ID | NJ-ART-03-2018-001223 |
| Article Type: | Paper |
| Date Submitted by the Author: | 12-Mar-2018 |
| Complete List of Authors: | Islam, Md; University of Texas at EL Paso, Chemistry<br>Ricardo, Saenz Arana; University of Texas at EL Paso, Chemistry<br>Wang, Huiyao ; New Mexico State University<br>Bernal, Ricardo; University of Texas at El Paso, Chemistry<br>Noveron, Juan; University of Texas at El Paso, Chemistry |
| | |

# Green synthesis of gold, silver, platinum, and palladium nanoparticles reduced and stabilized by sodium rhodizonate and their catalytic reduction of 4-nitrophenol and methyl orange

*Md. Tariqul Islam,*[a] *Ricardo Arana-Saenz,*[a] Huiyao Wang,[b] *Ricardo Bernal,*[a] *Juan C. Noveron.*[a]*

a. Department of Chemistry, University of Texas, El Paso, 500 West University Avenue, El Paso, Texas 79968, USA.

b. CURRL, New Mexico State University, 945 College Drive, Las Cruces, USA

* E-mail: jcnoveron@utep.edu

**Keywards:** gold nanoparticles, silver nanoparticles, platinum nanoparticles, palladium nanoparticles, sodium rhodizonate, catalytic reduction, 4-nitrophenol (4-NP), formic acid oxidation, methyl orange (MO) reduction.

## Abstract

Sodium rhodizonate was used as a bifunctional reducing as well as stabilizing agent for the single step synthesis of gold (Au), silver (Ag), platinum (Pt), and palladium (Pd) nanoparticles (NPs) in water. Transmission electron microscopy revealed that the Pt, Au, Ag, and PdNPs have the average core diameter of about 2, 8, 26, and 39 nm, respectively. The ability of these nanoparticles towards the catalytic reduction of 4-nitrophenol (4-NP) with sodium borohydride ($NaBH_4$) and the dual-catalytic oxidation of formic acid followed by the reduction of methyl orange (MO) was studied. The apparent rate constants ($k_{app}$), of the catalytic reduction of 4-NP in

the presence of Ag, Au, Pt, and PdNPs, were calculated to be 2.1482, 1.1167, 1.088 $\times 10^{-1}$, and 1.65 $\times 10^{-2}$ $min^{-1}$, respectively. However, for the dual-catalytic oxidation of formic acid followed by the reduction of MO, the $k_{app}$ were calculated to be 4.145, 1.25 $\times 10^{-2}$, 6.7 $\times 10^{-3}$, and 9.0 $\times 10^{-5}$ for the Pt, Pd, Au, and AgNPs, respectively.

**Introduction**

Noble metal nanoparticles possess unique size- and shape-dependent electrical, optical, chemical and physical properties.[1] Therefore, they are useful in variety of applications including chemical and biological sensing,[2] catalysis,[3] light harvesting,[4] bioimaging,[5] therapeutics,[6] and so on. In particular, their excellent catalytic properties, which is typically observed at the nanoscopic size in contrast to the macroscopic size, has made them some of the most widely studied nanomaterials.[7] As compared to the bulk material, the nanoparticles have larger proportion of atoms at the edges and the corners, which are surrounded by fewer atoms. The exposed atoms at the edges and the corners are considered to be chemically more reactive than the atoms in the bulk. Noble metal nanoparticles are reported to be used in a variety of catalytic reactions including, but not limited to the hydrogenation,[8] oxidation,[9] reduction,[10] coupling.[11] Recently, the catalytic reduction of 4-nitrophenol (4-NP) to 4-aminophenol (4-AP) and the dual-catalytic oxidation of the formic acid followed by the reductive degradation of organic pollutants have drawn much attention.[12,13] The catalytic reduction of 4-NP to 4-AP is not only a model reaction in academia but also the reduced product (4-AP) has industrial applications.[14] For example, 4-AP is used as a photographic developer, corrosion inhibitor, antioxidant, precursor for the manufacture of analgesic and antipyretic drugs, an intermediate in the synthesis of paracetamol, etc.[15] On the other hand, the dual-catalytic oxidation of the formic acid followed by the reductive degradation of organic pollutants is becoming an intriguing method in the area of

hydrogen storage and the environmental remediation.[15] The catalytic oxidation of formic acid generates $H_2$ and $CO_2$ gases. This reaction could be utilized as a clean and stable source of generating $H_2$ gas. Moreover, the in situ generated $H_2$ gas could be utilized to reductively degrade organic and inorganic pollutants in water viz. methyl orange, nitrate, and hexavalent chromium in water.[16] The formic acid induced reductive degradation of organic pollutants has benefit over other reducing agents *viz*. $NaBH_4$ as it does not produce any secondary pollutants. However, the catalytic reduction of the 4-NP and the dual catalytic oxidation of formic acid followed by the reductive degradation of MO commonly require noble metal nanoparticles as the catalysts.[17,18]

There are number methods for the synthesis of noble metal nanoparticles, where a wide variety reducing and/or stabilizing agents are utilized. For example, sodium citrate, [19] sodium borohydride, [20] thiols, sodium rhodizonate,[21] phosphine,[22] tripolyphosphate,[23] chitosan,[24] pyridine,[25] bipyridene,[26] amines,[27] fullerenes,[28] phthalocyanine,[29] carboxylic acid,[30] polyethylene glycol,[31] dendrimers,[32] plant extract,[33] etc. have been utilized as the reducing and/or stabilizing agents for the NPs synthesis. However, most of these methods cannot produce Au, Ag, Pt, and Pd nanoparticles following a common synthetic procedure. Further, some methods require multiple steps, harsh reducing agent *viz.* $NaBH_4$, organic solvents, prolonged stirring/incubation time, and separate reducing and stabilizing agents. Additionally, in the biological and medical drug delivery systems, chemical sensing of aqueous species, bio-imaging, and catalysis the requirement for the simplicity in the synthesis and water solubility is of the prime choice. Therefore, a generic and simple method for synthesis of noble metal nanoparticles using limited number of reagents is highly desired in the field of the noble metal nanoparticles research.

Herein, we report a general one-step method for the synthesis of Au, Ag, Pt, and PdNPs in water that are both reduced and stabilized by sodium rhodizonate. To the best of our knowledge, the ability of the rhodizonate ions for the synthesis of Au, Ag, Pt and PdNPs following a generic method has not been reported yet. The rhodizonate ion acts as a bifunctional reducing as well as stabilizing agent for the nanoparticles. UV-Vis spectroscopy, transmission electron microscopy (TEM), energy dispersive X-ray (EDX) spectroscopy, and the zeta potential measurements were used to characterize the NPs. The catalytic activities of the NPs were evaluated by two types of catalytic reactions. The first reaction studied here is the reduction of 4-NP to 4-AP in water in the presence of excess $NaBH_4$. The second reaction we studied here is the dual-catalytic oxidation of the formic acid followed by the reduction of MO.

## Materials and Methods

### Materials

Sodium rhodizonate dibasic (97%), hydrogen tetrachloroaurate trihydrate ($HAuCl_4{\cdot}3H_2O$, 99.9%), hydrogen hexachloroplatinate (IV) hydrate ($H_2PtCl_6{\cdot}3H_2O$ ≥99.9%), silver nitrate ($AgNO_3$), Palladium nitrate [$Pd(NO_3)_2$], 4-nitrophenol ($O_2NC_6H_4OH$ ≥99%), sodium borohydride ($NaBH_4$, 99%), formic acid ($CH_2O_2$) and methyl orange (MO), were purchased from Sigma-Aldrich, USA. Milli-Q water (>18.20 MΩ cm resistivity) was obtained from Milli-Q (Advantage A-10) water filter system.

### Characterization techniques

UV-Vis spectrum was obtained by using Agilent Cary 50 Conc UV-Visible Spectrophotometer using quartz cuvette of path length 10mm. Zeta potential measurement was carried out using Zetasizer Nano ZS90 with Disposable folded capillary cell. For the Zeta potential and UV-Vis analyses, 6 times diluted NPs solution in water was used. Low-resolution Transmission electron

microscopy (TEM) experiments were performed using a Hitachi H-7650 transmission electron microscope with an acceleration voltage of 80 kV. High- resolution Transmission electron microscopy (TEM) experiments were performed using a JEOL JEM3200FS Electron Microscope with an acceleration voltage of 300 kV. Carbon coated copper grids with 200 mesh (Electron Microscopy Science) were used for TEM imaging. 30 microliters of sample were deposited onto the grid and allowed to dry. IMAGEJ software was used to analyze average diameter and size distribution of AuNPs from the TEM images. Energy dispersive X-ray (EDX) analysis was carried out on dried AuNPs, which was centrifuged out at a speed of 15,000 rpm for 30 min. Hitachi S-3400N Type II scanning electron microscope (SEM) equipped with an energy dispersive X-ray spectrometer with accelerating voltage of 15 kV was used to obtain EDX spectrum. Glass substrate was used for the EDX analysis of AuNPs.

**Synthesis of the NPs in water**

All the nanoparticles were prepared following a same synthetic procedure. Separate 0.5 mM stock solutions of metal precursors were prepared by dissolving a required amount metal salt in water. A separate 9.7 mM aqueous solution of sodium rhodizonate was prepared by dissolving 83.04 mg (0.388 mmol) of sodium rhodizonate in 40 ml of water. For a typical synthesis, in a 100 mL round-bottomed flask 20 mL of 0.5 mM aqueous solution of metal precursor was allowed to boil. Afterwards, 4 mL of 9.7 mM sodium rhodizonate was injected while vigorous stirring of the solution. The reaction mixture was further boiled for 20 min to make sure a complete reduction of the metal ions. The molar ratio of the sodium rhodizonate to the noble metal ions was 3.88 in all the syntheses. The NPs solutions were preserved under ambient conditions for further characterization and catalytic applications.


**Scheme 1**. Synthesis of the Au, Ag, Pt, and PdNPs in water that are reduced and stabilized by sodium rhodizonate.

**Catalytic activity of the NPs**

The catalytic activity of the nanoparticles was evaluated by two different types of reduction reactions, Scheme 2 and 3. The first reaction was the reduction of 4-nitrophenol (4-NP) to 4-aminophenol (4-AP) in presence of excess $NaBH_4$, whereas the second reaction was the dual-catalytic oxidation of formic acid followed by the reduction of methyl orange.

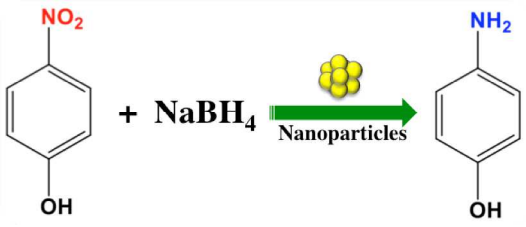


**Scheme 2.** Metal nanoparticles catalyzed reduction of 4-NP to 4-AP in presence of $NaBH_4$.

For the reduction of 4-NP, in a standard quartz cuvette 1 mL of 4-NP aqueous solution (0.2 mM) was mixed with 50 µL of NPs stock solution. Afterwards, 0.5 mL of freshly prepared

$NaBH_4$ aqueous solution (5mg $NaBH_4$ in 0.5 ml of water) was added into the quartz cuvette and the reaction course was monitored, every 30 second, by using the UV-Vis spectrophotometer. The UV-Vis spectrophotometer monitored the time-dependent lowering of the absorbance of 4-nitrophenolate at 400 nm. It is worth mentioning that the 4-NP reacts with $NaBH_4$ to yield 4-nitrophenolate, which shows strong absorption band centred at 400 nm.

For the dual-catalytic oxidation of formic acid followed by the reduction of MO, in a standard quartz cuvette, 50 µL of NPs stock solution was added to 1.5 mL of 26.7 ppm aqueous solution of MO. Afterwards, 50 µL of formic acid was added and mixed quickly. The reaction course was monitored by the UV-vis spectroscopy, which monitored the lowering of the absorbance of MO at 515 nm in every 30 s interval of time.

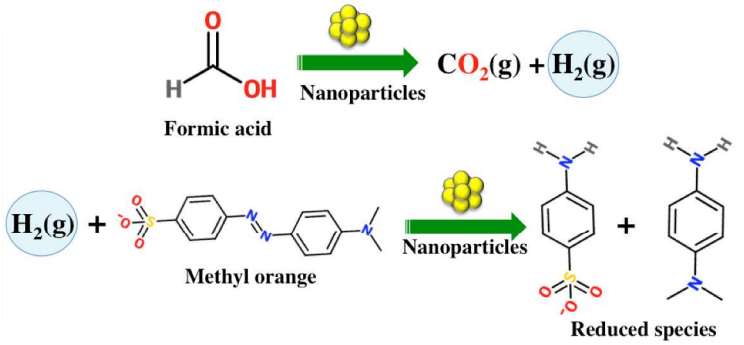


**Scheme 3.** Metal nanoparticles induced dual-catalytic oxidation of formic acid followed by the reduction of methyl orange (MO).

The percent reduction of 4-AP and MO was calculated using the following equation.[34]

$$\text{Percent reduction of 4-AP or MO} = \frac{A_0 - A_t}{A_0} \times 100\ \%$$

where $A_0$ and $A_t$ represent the absorbance of 4-NP and MO at 400 and 515 nm, respectively at the beginning and at time (t) of the catalytic reduction.

The reaction kintics was analyzed by the linear form of the pseudo-first-order kinetic model, which is expressed by the following equation.

Pseudo-first-order reaction rate equation, $-\ln \frac{C_t}{C_0} = kt$

where k (1/min) reprsents the pseudo-first-order rate constant of the catalytic reduction; $C_o$ and $C_t$ represent the initial and time-dependent concentrations of 4-NP and MO, respectively,

**Results and discussion**

The Au, Ag, Pt, and PdNPs were facilely synthesized by mixing solutions of sodium rhodizonate and metal precursor solutions in water at an elevated temperature. The reaction mixture changed color immediately after the solutions were mixed together. This indicated the formation of NPs by the naked eye visualization. The rhodizonate ions reduced the metallic ion to metallic NPs. Afterwards, the excess rhodizonate ions bound to the metallic ions situated on the surface of the nanoparticles by the coordination bond. As a result the rhodizonate ions capped the NPs from further growth. Therefore, the rhodizonate ions acted as the bifunctional reducing as well as capping agent. The ability of rhodizonate ion to form coordination complexes with different metal ions has been reported before.[35,36] However, its ability toward the reduction of Ag, Pt, and Pd ions to their metallic nanoparticles followed by their stabilization is not investigated until we reported here. Therefore, sodium rhodizonate could potentially be utilized as a soft reducing agent for various other organic syntheses, where reducing agent *viz.* $NaBH_4$ is too strong to use. Furthermore, the catalytic activity of the nanoparticles towards the reduction of 4-NP and the reductive degradation of MO is systematically studied and compared. The catalytic reduction of 4-NP is not only a model reaction that is commonly studied in academia but also the reduction

product has some industrial applications. The catalytic oxidation of formic acid followed by the reductive degradation of MO, on the other hand, could be utilized as a green method to degrade organic pollutants in water, which could be an attractive alternative method in the area of environmental remediation.

## Characterization of the NPs

### UV-Visible spectroscopy of the NPs

The typical UV-Vis spectrum of the Au, Ag, Pt, and PdNPs are shown in Figure 1. Strong absorption bands centered at about 530 and 416 nm were observed for the Au and AgNPs, respectively. This type of absorption band is also known as the surface-plasmon resonance (SPR) absorption band, which is usually exhibited by the Au and Ag nanoparticles.[37,38] The SPR band of the nanoparticles originates from the collective oscillation of conduction electrons upon interaction with electromagnetic radiation.[39] It could be observed that the SPR band generated by AgNPs is about 100 nm blue shifted compared to the AuNPs. This is because of the fact that the Ag and Au have completely different atomic size, electronic structure and conductivity.

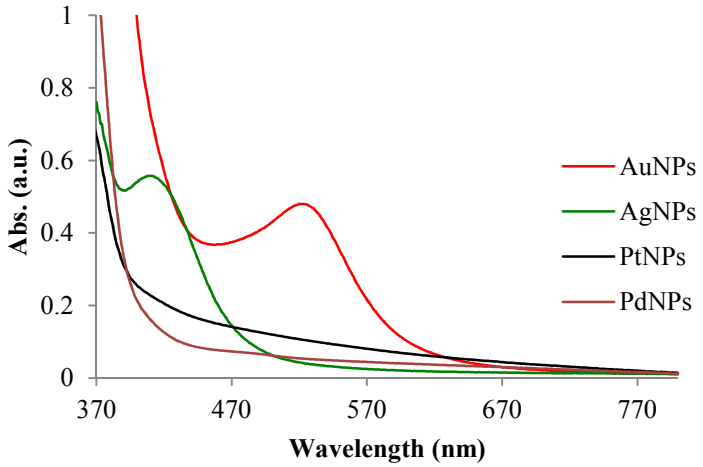


**Figure 1**. UV-Visible absorption spectrum of the Au, Ag, Pt, and PdNPs in water.

On the other hand, the Pt and PdNPs did not show any SPR band in the visible region of the electromagnetic radiation, which is similar to other reports.[40,41] The SPR band of platinum and palladium nanoparticles are usually found in the ultraviolet range, unlike the Au and AgNPs, which usually display SPR band in the visible region. Additionally, the size of the nanoparticles and their degree of aggregation usually shift the surface SPR band. For example, gold nanoparticles less than 2 nm in size usually do not exhibit the SPR band in the visible region.[42]

**TEM, HRTEM, EDS, and Zeta Potential of the NPs**

The typical TEM images of the NPs with the corresponding size distributions are shown in Figure 2. The TEM images show that the Au, Ag, and PtNPs are fairly spherical and well dispersed in in water although some degree of aggregations could also be observed. It could be observed that some of the AuNPs look like nanoprism and nanocube. The AgNPs are seen to be larger in diameter and have more faced morphology compared to the other NPs.

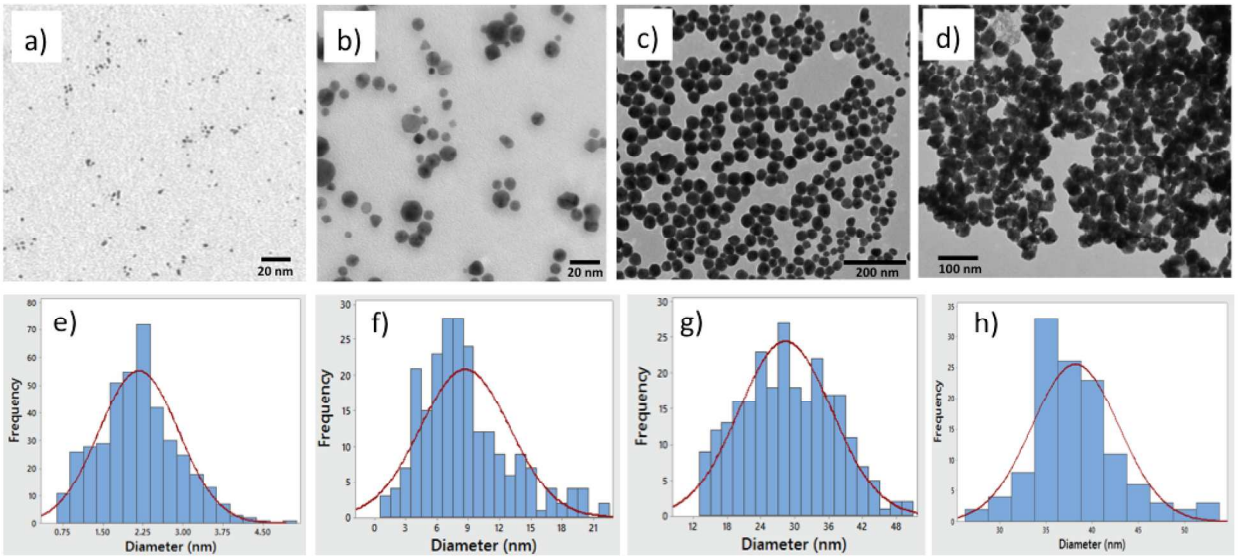

Figure 2. Typical TEM images of the a) PtNPs, b) AuNPs, c) AgNPs, and d) PdNPs. Corresponding size distributions of the NPs (e-h). Scale bar = 20, 20, 200 and 100 nm for the Pt, Au, Ag and PdNPs, respectively.

The PdNPs are observed to be somewhat less spherical and amorphous in shape. Moreover, the PdNPs were found to be more aggregated compared to the Au, Ag, and PtNPs in solution. The corresponding size distribution histograms of the NPs reveal that the Pt, Au, Ag, and PdNPs have the average core diameter of about 2, 8, 26, and 39 nm, respectively. The change in particles size could be attributed to the difference in the reduction potential of the metals and the stabilization ability of the rhodizonate ion towards the different noble metal ions studied here.

In order to determine the crystallinity as well as to analyze the nanoparticles qualitatively, high-resolution TEM analysis was carried out, Figure 3. HRTEM image can reveal the crystalline faces of the nanoparticles with atomic resolution. Moreover, the interlayer spacing, obtained from the HRTEM images, is usually utilized to characterize the different lattice planes of crystalline materials, which in turn is used for the qualitaive analysis of the material.

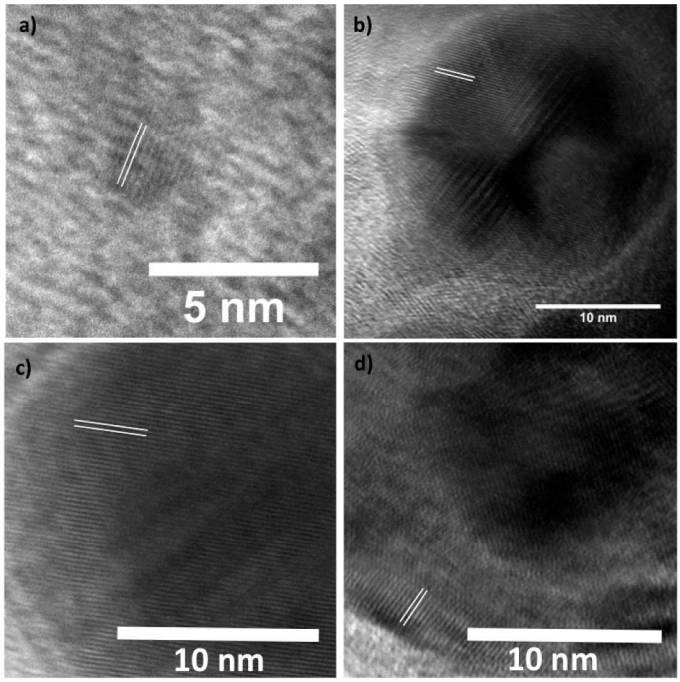


Figure 3. HRTEM images of the a) PtNPs, b) AuNPs, c) AgNPs, and d) PdNPs showing the characteristic (111) interlattice spacing

The interlayer spacing, shown in figure 3a, is measured to be about 0.22 nm, which is the characteristic lattice spacing of the platinum Pt(111) planes.[43] Similarly, the characteristic interlayer spacing of the Au(111), Ag(111), and Pd(111) planes were measured to be about 0.23, 0.24, and 0.22 nm, respectively, figure 3b-d.[44,45,46] Therefore, the HRTEM images confirmed the nanoparticles are crystalline and metallic in nature.

Energy-dispersive X-ray (EDX) analysis was conducted to determine the elemental composition of the nanoparticles. As a representative, the EDX spectrum was obtained from the AuNPs sample only, Figure 4a. The EDX spectrum revealed the presence of gold, carbon, and oxygen in the nanoparticles sample. The presence of carbon and oxygen indicate the presence of rhodizonate ions that are bound to the AuNPs surfaces. This further indicates that the stabilization of the AuNPs by the excess rhodizonate ions present in the solution.

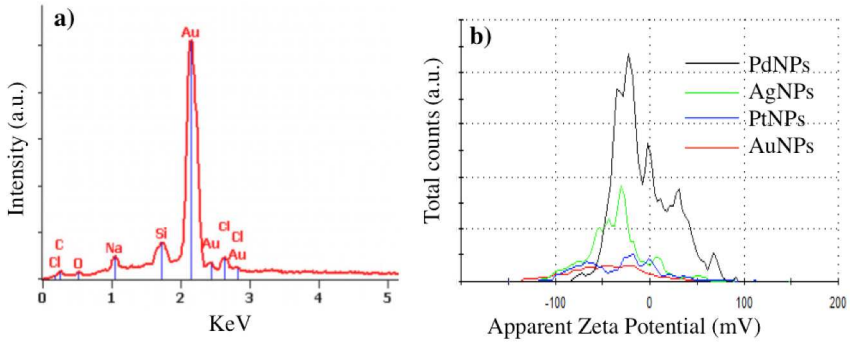


Figure 4 a) Energy dispersive X-ray (EDX) spectrum of AuNPs and b) Zeta potential of the AuNPs in water.

The zeta potential measurements were carried to determine the net charge on the NPs surface, Figure 4b. The net zeta potential was determined to be -32.7, -34.0, -20.5, and -7.46 for the Au, Ag, Pt, and PdNPs, respectively. The net negative values of the zeta potential further suggests the binding of the negatively charged rhodizonate ions on the nanoparticles surface and thereby yield a negative zeta potential. This indicates the dispersion stability of the NPs in water due to the interparticles electrostatic repulsive forces. Moreover, it could be observed that the PdNPs have the least net zeta potential value. This in turn indicates the poor dispersion stability of PdNPs in water in compared to the other NPs. This result is similar to the TEM studies, where the PdNPs were seen highly aggregated compared to the other NPs.

**Catalytic reduction of 4-nitrophenol by the NPs**

The time-dependent decrease in the absorbance of 4-NP centered at 400 nm with the corresponding kinetics of the catalytic reductions is shown in Figure 5. Figure 5a shows the continuous decrease in the absorbance of 4-NP at 400 nm during its catalytic reduction in presence of the AgNPs. The time-dependent percent reduction of the 4-NP, catalyzed by different NPs, is shown in Figure 5b. It could be observed that the Ag and AuNPs were faster catalyzing the reduction of 4-NP compared to the Pd and PtNPs. The un-catalyzed reaction,

where no NPs were used, shows negligible percent reduction of the 4-NP. This signifies the robust nature of 4-NP to undergo the reduction by $NaBH_4$ only. The slow catalytic activity of the PtNPs could be attributed to its strong stabilization by the rhodizonate ions in solution. However, the slow catalytic activity of the PdNPs could be attributed to its large particle size and high degree of aggregations in solution.

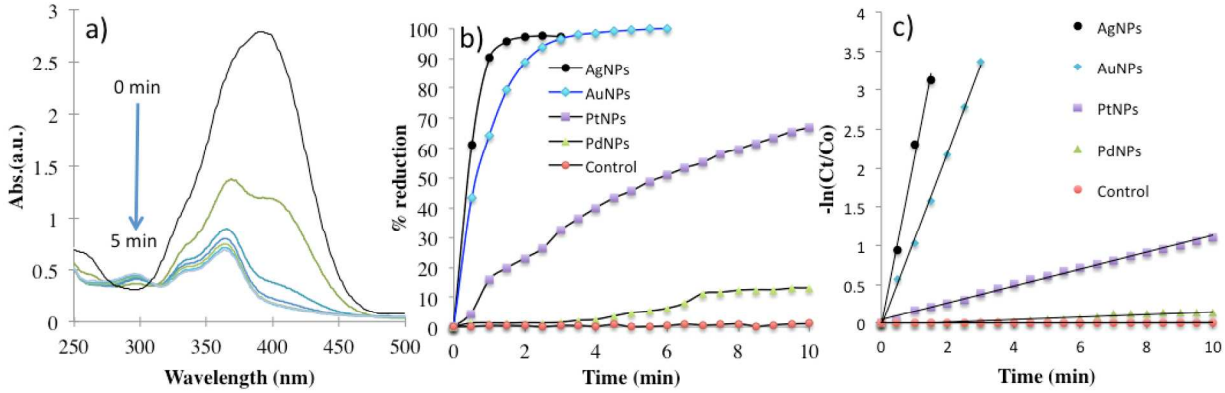


Figure 5 a) Time-dependent UV-vis absorption spectrum of the 4-NP reduction catalysed by the AgNPs, b) Time-dependent percent reduction of the 4-NP catalysed by different nanoparticles, and c) Pseudo-first order kinetics of the corresponding catalyzed and un-catalyzed reductions.

The kinetics of the catalytic reduction of 4-NP, catalysed by different NPs, is shown in Figure 5c. A linear relationship between the $-\ln(C_t/C_0)$ and reaction time (t) was observed. This suggests that the kinetics of the 4-NP reduction follows the Langmuir–Hinshelwood (LH) model. Moreover, the linear increase of $-\ln(C_t/C_0)$ with respect to the reaction time indicates that the reduction follows pseudo-first-order kinetics. The apparent rate constants ($k_{app}$), of the catalytic reduction of 4-NP in the presence of Ag, Au, Pt, and PdNPs were found to be 2.1482, 1.1167, 1.088 $\times 10^{-1}$, and 1.65 $\times 10^{-2}$ $min^{-1}$, respectively. Whereas, the apparent rate constant of the un-catalyzed reaction is calculated to be 8.0 $\times 10^{-4}$ $min^{-1}$. Moreover, it could be observed that the

induction time for the Ag and AuNPs catalyzed reaction is about zero, which indicate their fast catalytic activity.

**Catalytic oxidation of formic acid followed by the reduction of MO**

Figure 6 shows the time-dependent decrease in the absorbance of MO centered at 515 nm with the corresponding kinetics of the reduction. Likewise the 4-NP reduction, the –ln(Ct/Co) vs time (t) is a straight line, which indicates that the reactions follow pseudo-first-order kinetics. The apparent rate constants of the reactions are calculated to be 4.145, 1.25 $\times 10^{-2}$, 6.7 $\times 10^{-3}$, 9.0 $\times 10^{-5}$ and 7.0 $\times 10^{-5}$ $min^{-1}$, for PtNPs, PdNPs, AuNPs, AgNPs catalysed and control experiments, respectively. The un-catalyzed reaction, where no NPs were used, showed negligible percent reduction of the MO. The PtNPs demonstrated very fast and the Pd and AuNPs demonstrated moderate catalytic activity, whereas the AgNPs showed negligibl activity under the experimental conditions.

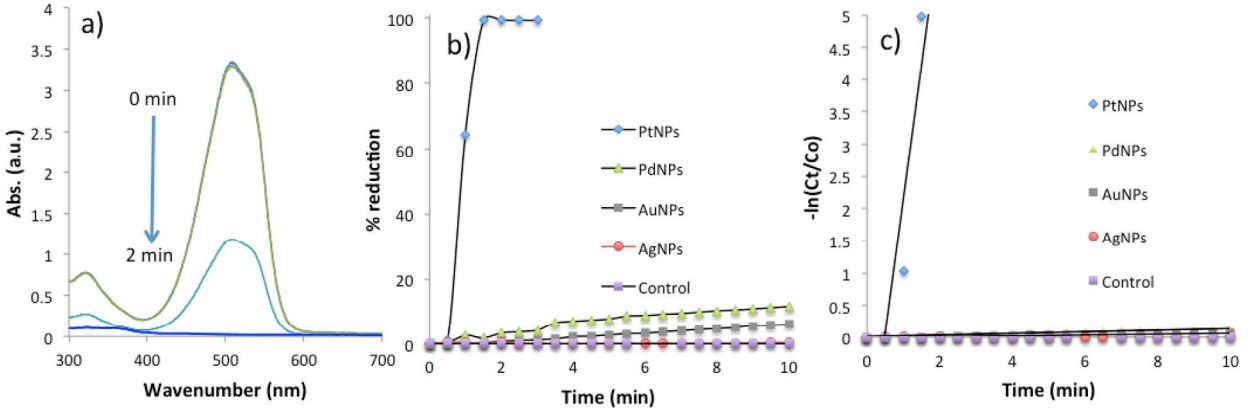


Figure 6. a) Time-dependent UV-vis absorption spectrum of the MO reduction catalysed by the PtNPs; b) Time-dependent % reduction of the MO catalysed by different nanoparticles, and c) Pseudo-first order kinetics [$-\ln(C_t/C_0)$ vs. reaction time (t)] curves for the catalytic reduction of MO

The Pt and the PdNPs are well-known catalysts for the oxidation of formic acid to generate $CO_2$ and $H_2$ gases.[47] Afterwards, the $H_2$ gas gets chemisorbed on the NPs surface, which eventually reduces the MO and break the conjugation through the diazo (N=N) bond. As a result the MO looses its color gradually. The slow catalytic activity of the PdNPs, in this study, could be attributed to their large particle size and high degree of aggregations in solution. Moreover, it could be observed that the induction period for the PtNPs catalyzed reaction is about 30 sec. This may happen due to the two steps catalysis reactions *viz.* the oxidation of formic acid and the reduction of the MO. Induction period is commonly observed in heterogeneous catalysis and it is a measure of the time that takes to reach the adsorption-desorption equilibrium between the reactants and products with the catalyst.

**Conclusions**

In conclusion, we report a facile method for the generation of Au, Ag, Pt and Pd nanoparticles in water that are both reduced and stabilized by sodium rhodizonate. The performance of these nanoparticles towards the catalytic reduction of 4-nitrophenol (4-NP) and methyl orange (MO) was systematically studied and compared. The results indicated that AgNPs followed by AuNPs exhibited significantly faster kinetics for the reduction of the 4-NP with $NaBH_4$ as compared to the Pt and the PdNPs. In contrary, the reduction of MO with formic acid catalyzed by the Pt and PdNPs was found to be faster as compared to the AuNPs and AgNPs. Sodium rhodizonate mediated synthesis of the Au, Ag, Pt and Pd nanoparticles represent a general route for functionally active catalysts with a wide range of potential applications.

**Author Information**

Corresponding Author: Juan C. Noveron

*E-mail: jcnoveron@utep.edu

## Notes

The authors declare no conflicting financial interest.

## Acknowledgement

Financial support from NSF grants CHE-0748913, MRI-0923437, DMR PREM-1205302, the NEWT-1449500, and USDA 2014-38422-22078 are gratefully acknowledged. We thank Dr. Jorge Gardea-Torresdey research group for their kind assistance with the Zeta-potential measurements.

## References

[1] M. C. Daniel and D. Astruc, Chem. Rev., 2004, **104**,1.

[2] K.Saha, S. S. Agasti, C. Kim, X. Li and V. M. Rotello, Chem. Rev., 2012, **112**, 5.

[3] M. T. Islam, J. E. Padilla, N. Dominguez, D. C. Alvarado, M. S. Alam, P. Cooke, M. M. J. Tecklenburg and J. C. Noveron, RSC Adv., 2016, **6**, 94.

[4] S. Pillai, K. R. Catchpole, T. Trupke and M. A. Green, J. Appl. Phys., 2007, **101**, 9.

[5] L. Dykman and N. Khlebtsov, Chem. Soc. Rev. 2012, **41**, 6.

[6] L. C. Cheng, J. H. Huang, H. M. Chen, T. C. Lai, K. Y. Yang, R. S. Liu and D. P. Tsai, J. Mater. Chem., 2012, **22**, 5.

[7] S. Eustis and M. A. El-Sayed, Chem. Soc. Rev., 2006, **35**, 5.

[8] T. Mitsudome and K. Kaneda, Green Chem. 2013, **15**, 10.

[9] M. Haruta, Catal. Surv. Asia, 1997, **1**, 1.

[10] M. Guo, J. He, Y. Li, S. Ma and X. Sun, J. Hazard. Mater. 2016, **310**, 89-97.

[11] B. Karimi, M. Gholinejad and M. Khorasani, Chem. Commun. 2012, **48**, 71.

[12] B. Zheng, X. Liu, Y. Wu, L. Yan, J. Du, J. Dai, Q. Xiong, Y. Guo and D. Xiao, Inorg. Chem. Front., 2017, **4**, 8.

[13] M. Nasrollahzadeh, M. Sajjadi, M. Maham, S. M. Sajadi and A. A. Barzinjy, Mater. Res. Bulletin, 2018, **102**, 24–35

[14] S. Mehmood, N. K. Janjua, F. Saira and H. Fenniri, J. Spectrosc., 2016.

[15] L. Zhang, Y. Guo, A. Iqbal, B. Li, M. Deng, D. Gong, W. Liu and W. Qin, J. Nanopart. Res., 2017, **19**, 4.

[16] P. Veerakumar, P. Thanasekaran, K. C. Lin and S. B. Liu, ACS Sust. Chem. Eng., 2017, **5**. 6.

[17] Y. Shao, L. Zhou, C. Bao, Q. Wu, W. Wu and M. Liu, New J. Chem., 2016, **40**, 11.

[18] N. G. Patil, N. B. Basutkar, and A. V. Ambade, New J.Chem., 2017,**41**,11.

[19] J. Turkevitch, P. C. Stevenson and J. Hillier, Discuss. Faraday Soc. 1951, **11**, 55-75.

[20] M. Brust, M. Walker, D. Bethell, D. J. Schiffrin and R. Whyman, J. Chem. Soc., Chem. Commun., 1994, **801**, 3.

[21] M. T. Islam, N. Dominguez, M. A. Ahsan, H. Dominguez-Cisneros, P. Zuniga, P. J. Alvarez, and J. C. Noveron, J. Environ. Chem. Eng., 2017, **5**, 5.

[22] W. W. Weare, S. M. Reed, M. G. Warner and J. E. Hutchison, J. Am. Chem. Soc., 2000, **122** 51.

[23] J. Xin, L. Miao, S. Chen and A. Wu, Anal. Methods, 2012, **4**, 5.

[24] H. Huang and X. Yang, Biomacromolecules, 2004, **5**, 6.

[25] V. J. Gandubert and R. B. Lennox, Langmuir, 2005, **21**, 14.

[26] P. M. Shem, R. Sardar and J. S. Shumaker-Parry, J. Colloid Interface Sci., 2014, **426**, 107-116.

[27] M. Aslam, L. Fu, M. Su, K. Vijayamohanan and V. P. Dravid, J. Mater. Chem., 2004, **14**, 12.

[28] M. T. Islam, S. K. Molugu, P. H. Cooke and J. C. Noveron, New J. Chem., 2015, **39**, 8.

[29] D. C. Hone, P. I. Walker, R. Evans-Gowing, S. FitzGerald, A. Beeby, I. Chambrier, M. J. Cook and D. A. Russell, Langmuir, 2002, **18**, 8.

[30] B. Mondal, N. Kamatham, S. R. Samanta, P. Jagadesan, J. He and V. Ramamurthy, Langmuir, 2013, **29**, 41.

[31] K. Rahme, L. Chen, R. G. Hobbs, M. A. Morris, C. O'Driscoll and J. D. Holmes, RSC Adv., 2013, **3**, 17.

[32] H. Liu, Y. Xu, S. Wen, Q. Chen, L. Zheng, M. Shen, J. Zhao, G. Zhang and X. Shi, Chem. Eur. J., 2013, **19**, 20.

[33] A. K. Mittal, Y. Chisti and U. C. Banerjee, Biotechnol. Adv., 2013, **31**, 2.

[34] M. T. Islam, C. Hernandez, M. A. Ahsan, A. Pardo, H. Wang and J. C. Noveron, J. Environ. Chem. 2017, **5**, 5.

[35] C. C. Wang, C. T. Kuo, P. T. Chou and G. H. Lee, Angew. Chem. Int. Ed. 2004, **43**, 34.

[36] A. Vogler, Inorg. Chem. Commun. 2016, **74**, 90-92.

[37] I. Diez and R. H. Ras, Nanoscale, 2011, **3**, 5.

[38] P. C. Ray, Chem. Rev. 2010, **110**, 9.

[39] C. Langhammer, Z. Yuan, I. Zorić and B.Kasemo, Nano Lett., 2006, **6**,4.

[40] A. Watanabe, M. Kajita, J. Kim, A. Kanayama, K. Takahashi, T. Mashino and Y. Miyamoto, Nanotechnology, 2009, **20**, 45.

[41] T. Teranishi and M. Miyake, Chem. Mater.,1998, **10**, 2.

[42] T. Shimizu, T. Teranishi, S. Hasegawa and M. Miyake, J. Phys. Chem. B., 2003, **107**, 12.

[43] K. Siuzdak, M. Sawczak, M. Klein, G. Nowaczyk, S. Jurga and A. Cenian, Phys. Chem. Chem. Phys., 2014, **16**, 29.

[44] S. Singh, R. Pasricha, U. M. Bhatta, P. V. Satyam, M. Sastry, B. L. V. Prasad, J. Mater. Chem., 2007, **17**, 16.

[45] A. E. Hernández-Gómora, E. Lara-Carrillo, J. B. Robles-Navarro, R. J. Scougall-Vilchis, S. Hernández-López, C. E. Medina-Solís and R. A. Morales-Luckie, Molecules, 2017, **22**, 9.

[46] E. Coronado, A. Ribera, J. García-Martínez, N. Linares and L. M. Liz-Marzán, J. Mater. Chem. 2008, **18**, 46.

[47] V. Grozovski, J. Solla-Gullón, V. Climent, E. Herrero, J. M. Feliu, J. Phys. Chem. C., 2010, **114**, 32.

Graphical abstract

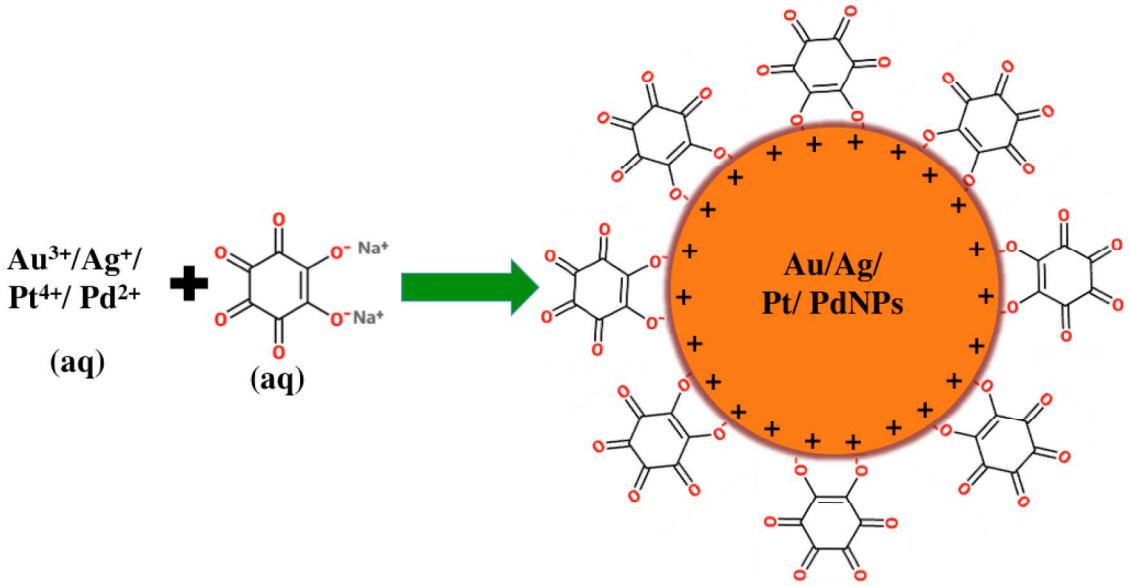


Sodium rhodizonate mediated green synthesis of gold, silver, platinum, and palladium nanoparticles and their catalytic reduction of 4-nitrophenol and methyl orange